A Journal of the Gesellschaft Deutscher Chemiker

# Angewandte International Edition Chemie

www.angewandte.org

2017–56/16

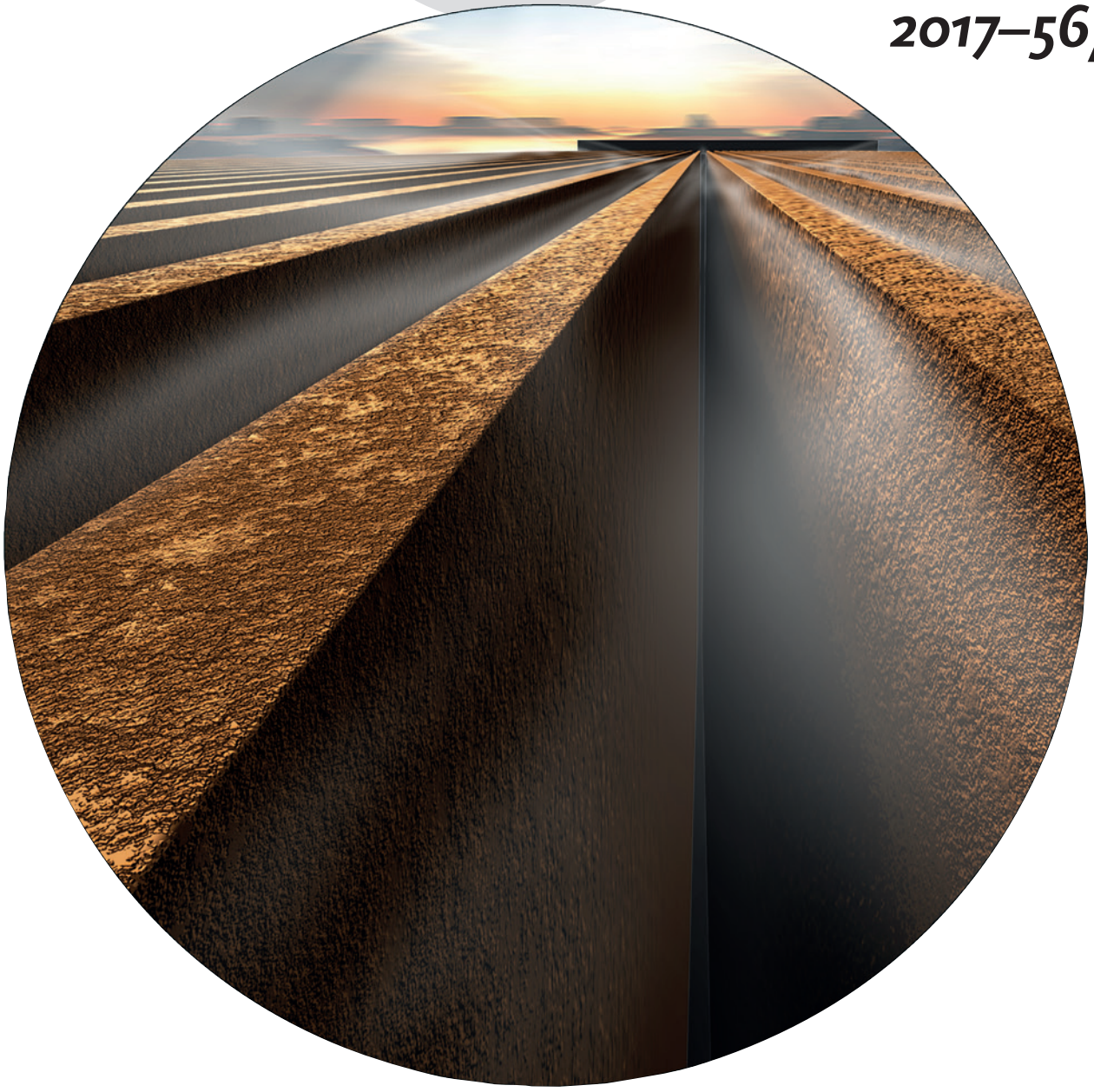

**Cover Picture**

*Z. Lin et al.*

Harnessing Colloidal Crack Formation by Flow-Enabled Self-Assembly

*ACIEFS 56 (16) 4363–4630 (2017) · ISSN 1433–7851 · Vol. 56 · No. 16*

150 Years GDCh

WILEY-VCH

Colloidal Microchannel | Very Important Paper

International Edition: DOI: 10.1002/anie.201700457
German Edition: DOI: 10.1002/ange.201700457

# Harnessing Colloidal Crack Formation by Flow-Enabled Self-Assembly

*Bo Li, Beibei Jiang, Wei Han, Ming He, Xiao Li, Wei Wang, Suck Won Hong, Myunghwan Byun, Shaoliang Lin, and Zhiqun Lin**

***Abstract:*** *Self-assembly of nanomaterials to yield a wide diversity of high-order structures, materials, and devices promises new opportunities for various technological applications. Herein, we report that crack formation can be effectively harnessed by elaborately restricting the drying of colloidal suspension using a flow-enabled self-assembly (FESA) strategy to yield large-area periodic cracks (i.e., microchannels) with tunable spacing. These uniform microchannels can be utilized as a template to guide the assembly of Au nanoparticles, forming intriguing nanoparticle threads. This strategy is simple and convenient. As such, it opens the possibility for large-scale manufacturing of crack-based or crack-derived assemblies and materials for use in optics, electronics, optoelectronics, photonics, magnetic device, nanotechnology, and biotechnology.*

In stark contrast to conventional top-down approaches, bottom-up self-assembly is widely recognized as a robust means of spontaneously organizing nanoscopic building blocks[1] into highly ordered structures and materials[2] for use in catalysis, optics, electronics, photonics, and sensors at remarkably low cost.[3] An exciting variety of self-assembled structures composed of many different kinds of nanomaterials as building blocks (e.g., DNA,[4] inorganic nanoparticles,[5] and block copolymers[4b,6]) have been created. In particular, colloidal cracks formed upon the drying and consolidation of colloidal suspension can also be considered as a self-organized assembly. Generally, cracks are strongly unfavorable and regarded as a problematic and challenging issue in the paint and coating industry, whereas a thin layer of film with uniform thickness is highly desired.[7] The cracks formed usually exhibit random and irregular morphologies (e.g., network and logarithmic spirals[8]) arising from the free drying of the liquid front. Surprisingly, despite that theoretical modeling for understanding the mechanism of crack formation have been extensively studied,[9] effective methods to experimentally manipulate cracks upon drying to provide new levels of tailorability to the morphology and regularity of cracks are comparatively few and limited in scope.[10] This may be due largely to the lack of control over the drying process.

In this context, recent research has witnessed rapid advances in controlling solvent evaporation by imposing confined geometries over droplets to create a myriad of regular structures and hierarchical assemblies consisting of, for example, block copolymers, DNA, quantum dots, carbon nanotubes. This contrasts sharply to conventional sessile droplet evaporation. Several confined geometries that render the delicate control over the evaporation process (e.g., evaporative flux, interfacial interaction between solute and substrate) have been rationally designed and implemented,[11] including cylindrical tubes,[12] two crossed cylinders,[13] two parallel plates,[14] lithographic mask,[15] and curve-on-flat configuration.[16] The ability to enable the controlled evaporative self-assembly of solution containing nonvolatile solutes situated in confined geometries as noted above may afford the precise regulation of the formation and propagation of colloidal cracks.

Herein, we report on a robust flow-enabled self-assembly (FESA) strategy to effectively harness the formation colloidal cracks by drying a colloidal suspension in a restricted geometry composed of a stationary upper blade over a movable lower substrate mounted on a computer-controlled translational stage. Intriguingly, large-area, highly ordered colloidal cracks with tunable spacing between two adjacent cracks $\lambda_{c-c}$ were reproducibly created. The formation of cracks was a direct consequence of capillary stress (stresses arising from the fluid–fluid tension[17]) generated during the drying of the colloidal thin film formed. By judiciously varying the moving velocity of the lower substrate at certain temperature and suspension concentration, the thickness of colloidal thin film can be readily tailored, thereby offering good control over the spacing between cracks. Moreover, the influence of chemically patterned substrate (i.e., hydrophobic polymer stripes on a hydrophilic substrate) on shaping colloidal cracks was explored. Subsequently, as these colloidal cracks existed in the form of microchannels with varied yet easily accessible spacings, they were exploited as template for directing the assembly of inorganic nanoparticles. Clearly, the

[*] B. Li, B. Jiang, Dr. W. Han, Dr. M. He, X. Li, W. Wang, Prof. Z. Lin
School of Materials Science and Engineering
Georgia Institute of Technology
Atlanta, GA 30332 (USA)
E-mail: zhiqun.lin@mse.gatech.edu
Prof. S. W. Hong
Department of Cogno-Mechatronics Engineering, Department of Optics and Mechatronics Engineering, Pusan National University
Busan 46241 (Republic of Korea)
Prof. M. Byun
Department of Advanced Materials Engineering
Keimyung University
Daegu 704-701 (Republic of Korea)
Prof. S. Lin
School of Materials Science and Engineering, East China University of Science and Technology
Shanghai 200237 (China)
Supporting information and the ORCID identification number(s) for the author(s) of this article can be found under: http://dx.doi.org/10.1002/anie.201700457.

  

FESA strategy is appealing because of its ability to engineer the crack formation in a simple and controllable manner and enable useful crack-based or crack-derived structures and systems for potential applications in lithography mask, photonics, electronics, separation, microfluidics and sensors.[18]

The polystyrene (PS) latex particle suspension at a concentration of 0.5 wt% was prepared by diluting 50-nm PS latex suspension (purchased from Thermo Scientific) with deionized water at 1:1 volume ratio. The droplet containing the PS nanoparticle suspension was then allowed to dry in a restricted geometry comprising a stationary glass upper blade placed over a movable lower substrate (i.e., Si wafer) fixed on a computer-controlled translational stage (Figure 1 and Figure S1 in Supporting Information). As a result of the "coffee-ring" effect,[19] the evaporative loss of water that was maximized at the three-phase contact line resulted in a lateral flow within the droplet, thereby transporting PS nanoparticles to the drying front. Subsequently, by continuously moving the lower Si substrate, the PS colloidal thin film disrupted by periodically spaced channel-like microscopic cracks (hereafter referred to as microchannels) on Si substrate was formed (i.e., a flow-enabled self-assembly (FESA) process). The direction of microchannels was parallel to the moving direction of the lower Si substrate. The moving velocity of Si substrate was set to be 13 $\mu m\,s^{-1}$ and the Si substrate was heated and maintained at 50 °C during the drying process (Figure 1). Notably, a droplet of 60 μL PS latex particle suspension yielded uniform microchannels over a surface area of $1 \times 1.5\ cm^2$ (width × length), which is dictated by the size of the stationary upper blade used in the FESA process ($1 \times 1.5\ cm^2$ in the present study) and the volume of the PS latex particle suspension, respectively. Clearly, a colloidal thin film with highly ordered microchannels over a much larger surface area can be readily achieved by capitalizing on an upper blade with a much larger size and continuously feeding the FESA apparatus with the PS latex particle suspension.

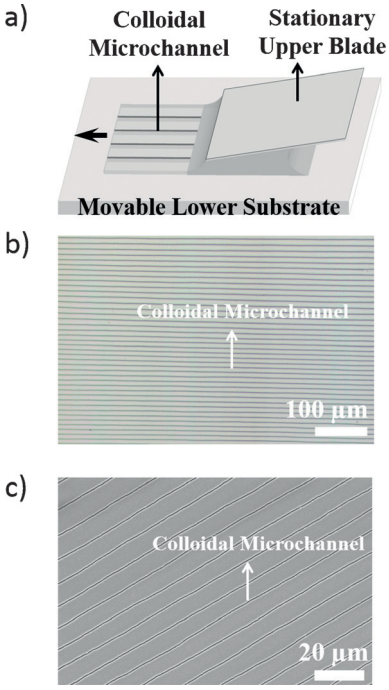


***Figure 1.*** a) Schematic illustration of the formation of uniform microscopic cracks (i.e., microchannels) by flow-enabled self-assembly (FESA) of the polystyrene (PS) latex particle suspension. The upper blade was fixed while the lower Si substrate was moved at a constant velocity of 13 $\mu m\,s^{-1}$ during the entire drying process. b) Representative optical micrograph of microchannels. c) Representative SEM image of microchannels. The concentration of the PS latex particle water solution prepared by diluting 50-nm PS latex particle suspension with DI-water at 1:1 volume ratio was 0.5 wt%, and the temperature of the lower Si substrate was 50 °C.

It is interesting to note that the spacing between two adjacent microchannels ($\lambda_{c-c}$), ranging from 7.8 μm to 38.7 μm obtained in our experiments, was much smaller than those reported by freely drying a droplet of particle suspensions on a substrate (i.e., drying of a sessile droplet), which are usually more than 200 μm.[20] Thus, the FESA strategy developed in the study effectively makes the creation of uniform microchannels with roughly an order of magnitude smaller feature size. Importantly, $\lambda_{c-c}$ can be easily tuned by simply varying the moving velocity of the regular colloidal microchannels (Figure 2a). The formation of cracks (i.e., microchannels) is mainly governed by the capillary stress generated during the drying of the colloidal thin film.[21] The $\lambda_{c-c}$ can be given by [Eq. (1)][22]

$$\lambda_{c-c} \approx 0.07\left(\frac{20}{75}\left(\frac{3\gamma\eta_0}{E}\right)^{\frac{1}{2}}\frac{R(1-\phi)^2}{\mu\phi^2 H}\right)^{-0.8}\left(\frac{20R(1-\phi)^2}{75\mu\phi^2}\right)\left(\frac{3\gamma^3\eta_0}{E^3}\right)^{\frac{1}{4}} \quad (1)$$

where $\gamma$ is the surface tension of water, $\eta_0$ is the dispersion viscosity of water into colloidal thin films, $E$ is the evaporation rate, $R$ is the radius of colloidal nanoparticle, $\phi$ is the volume fraction of colloidal nanoparticle, $\mu$ is the viscosity of water, and $H$ is the thickness of the dried colloidal film. As the same

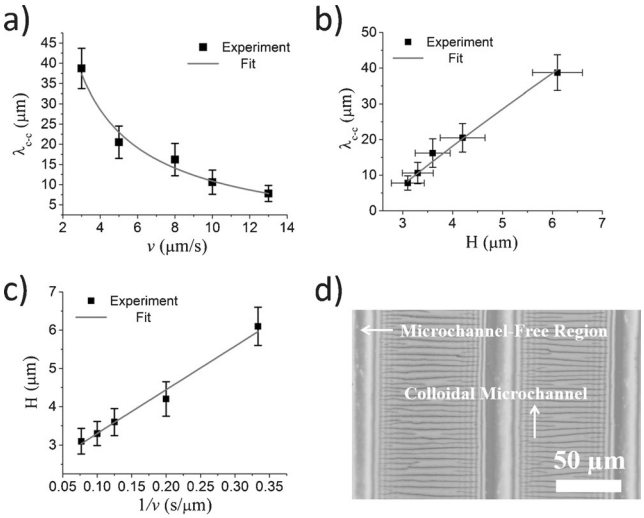


***Figure 2.*** Experimental results and theoretical prediction of the relationships of a) the spacing between adjacent microchannels $\lambda_{c-c}$ and the moving velocity of the lower Si substrate $v$, b) $\lambda_{c-c}$ and the thickness of the dried colloidal thin film $H$, and c) $H$ and $1/v$. d) Representative optical micrograph of the colloidal thin film with a thickness lower than a critical value, in which the microchannels appear to be discontinued and the microchannel-free regions emerged.

  

PS latex particle was used and the other experimental parameters were kept unchanged (i.e., temperature, solution concentration, and solvent), thus the $\lambda_{c-c}$ in Equation (1) can be simplified as [Eq. (2)]

$$\lambda_{c-c} \approx kH^{0.8} \quad (2)$$

where $k$ is the constant, including all other parameters mentioned in Equation (1). It is noteworthy that the fitted curve using Equation (2) correlated well with the experimental results (Figure 2b), which is also in good agreement with the theoretical prediction in the literature that $\lambda_{c-c}$ almost increased linearly with the thickness of the dried colloidal thin film $H$ with a slight deviation.[9a] The total volume of PS nanoparticles V deposited from the drying front can be given by [Eq. (3)]

$$V = lhd \approx \frac{4}{3}\pi R^3 \alpha t = \frac{4\pi R^3 \alpha d}{3v} \quad (3)$$

where $l$, $h$ and $d$ are the width, thickness, and length of the wet colloidal thin film prior to cracking, respectively, $\alpha$ is PS latex particles deposition rate at the contact line per unit time, $t$ is the time period of the FESA process, and $v$ is the moving velocity of the lower Si substrate. Clearly, the length of the colloidal thin film equals to the moving distance of substrate at the given time $t$. The thicknesses of colloidal film before and after drying should be in a linear relationship as the number of PS latex particles did not change during drying (i.e., $H \approx h$). Moreover, $h$ can be directly correlated with v (i.e., $h \approx 4\pi R^3\alpha/3vl$) based on Equation (3). Thus we have $H \approx 4\pi R^3\alpha/3vl$. Assuming that the deposition rate of PS latex particles $\alpha$ is independent of $v$, thus, $H$ is inversely proportional to $v$, which was also observed in our experiments (Figure 2c). Taken together, according to Equation (2), we have[Eq. (4)]

$$\lambda_{c-c} \approx k\left(\frac{4\pi R^3\alpha}{3vl}\right)^{0.8} \approx k'v^{-0.8} \quad (4)$$

where $k' = k(4\pi R^3\alpha/3l)^{0.8}$. It is worth noting that the fitted curve based on Equation (4) and the experimental results agreed well with one another (Figure 2a). Therefore, the experimental observation of the relationship between $\lambda_{c-c}$ and $v$ shown in Figure 2a can be well understood. In addition, it has been reported that there exists a critical thickness for crack-free (i.e., microchannel-free) thin film, above which colloidal microchannels form.[23] Importantly, such a critical thickness was also found in our work. By increasing the moving velocity of the lower Si substrate above 13 μm s$^{-1}$ (e.g., 15 μm s$^{-1}$), the colloidal film with discontinued microchannels (i.e., the microchannel-free regions) was observed at the thickness below 3.1 μm (Figure 2d). We note that the thickness of the colloidal thin film which is strongly determined by the deposition rate of PS latex particles α can also be tuned linearly by varying the concentration of the PS latex particle suspension and the temperature. Thus, the colloidal film with microchannel-free regions shown in Figure 2d were also observed at lower temperature of the lower Si substrate (e.g., 45 °C; Figure S3a) or at the lower solution concentration (e.g., 0.2 wt %; Figure S3b), while the other parameters were kept the same as those in Figure 1.

We also investigated the influence of a chemically patterned substrate on the crack formation. The chemically patterned substrate composed of regularly spaced hydrophobic PS homopolymer stripes on hydrophilic Si substrate was prepared by FESA of the PS homopolymer toluene solution using the same apparatus described above. Specifically, similar to our previous work,[14b] these PS stripes were created via a controlled "stop-and-move" motion of the lower Si substrate during the FESA process. First, the Si substrate was moved for a desired distance rendered by computer-controlled translation stage. It was then stopped for a certain time to deposit PS at the pinned three-phase contact line. The Si substrate was then moved again, leaving behind a PS stripe. The repetitive "stop-and-move" cycles of the lower Si substrate yielded precisely spaced PS stripes. Notably, the height of PS stripe and the spacing between adjacent PS stripes can be readily manipulated by controlling the deposition time at the "stop" stage and the distance that the lower Si substrate moved at the "move" stage, respectively, during FESA.[14b] Nonetheless, these regularly spaced hydrophobic PS stripes on hydrophilic Si substrate were exploited as the chemically patterned substrate. Subsequently, a drop of PS latex particle suspension ($c = 0.5$ wt %, dispersed in water as noted above) was allowed to dry in this new restricted geometry consisting of a stationary upper blade and a lower movable chemically patterned substrate (i.e., a FESA process). The moving direction of the lower chemically patterned substrate was set to be perpendicular to the PS stripes. Unless otherwise specified, the temperature, the moving velocity of the lower substrate, and the concentration for the FESA of PS latex particle suspension on the chemically patterned substrate were 50 °C, 13 μm s$^{-1}$, and 0.5 wt %, respectively. For the PS stripes with smaller height ($h \approx 3$ μm) and longer spacing between adjacent stripes ($d_{S-S} = 100$ μm), colloidal thin film with microchannels still formed (Figure 3a,b), similar to that produced on the bare Si substrate (Figure 1). However, the microchannels were interrupted by the PS stripe and then continued afterward (Figure 3b and Figure S4a). Quite intriguingly, despite occurring at a much smaller scale (ca. 100 nm wide, Figure S4b), the PS stripes themselves were also cracked caused by the formation of two adjacent large-sized microchannels (i.e., cracks ca. 800 nm wide). Subsequent microchannels were continued to form under the guidance of the smaller cracks built within PS stripes. In the previous report,[9a] the crack opening stress of colloidal film was predicted to be several MPa, which would not be sufficient to crack the PS stripe (the Young's modulus of PS is ca. 3 GPa[24]) in this work. Our experimental results (Figure S4b) indicates that the theoretical prediction[9a] may underestimate the crack opening stress of colloidal film.

Surprisingly, for the PS stripes with larger height ($h \approx 5$ μm) and shorter spacing between adjacent stripes ($d_{S-S} = 50$ μm), colloidal thin film was not formed (Figure 3c and d). On the basis of in situ optical microscopy observation, this may be understood as follows. Compared to the case described above ($h \approx 3$ μm and $d_{S-S} = 100$ μm), as the distance

  

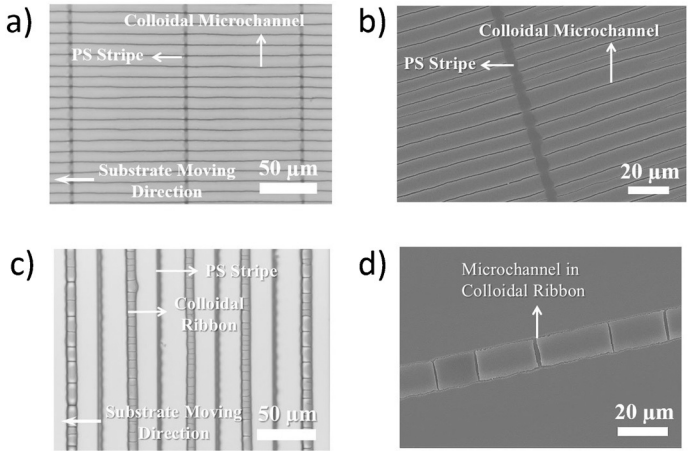


***Figure 3.*** a) Optical micrograph and b) SEM image of cracks (i.e., microchannels) formed on the periodically spaced PS stripes ($h \approx 3$ μm, $d_{S-S} = 100$ μm) by controlled drying of the PS latex particle suspension during the FESA process. The lower Si substrate was moved in a direction (i.e., the same direction as the produced microchannels) perpendicular to the patterned PS stripes. The microchannels were formed over the entire substrate except on the top of PS stripes. c) Optical micrograph of colloidal ribbons and d) SEM image of colloidal ribbon with cracks (microchannels) created within yet normal to it. Similar to (a) and (b), the colloidal ribbons were also formed on chemically patterned PS stripes but with a larger height of stripe ($h \approx 5$ μm) and a shorter distance between adjacent stripes ($d_{S-S} = 50$ μm). The lower Si substrate was also moved in a direction perpendicular to the patterned PS stripes (i.e., perpendicular to the formed colloidal ribbons, and parallel to the produced microchannels that are within the ribbon).

between adjacent hydrophobic PS stripes decreased from 100 μm to 50 μm, the area of exposed hydrophilic Si substrate, on which the PS latex particle water solution (i.e., the suspension in water) would preferentially wet to form a colloidal film, was thus considerably reduced. As a result, although the lower PS-stripes-deposited Si substrate was moved continuously at a constant velocity, the three-phase contact line of the evaporating droplet was slipped from the front PS stripe and pinned in the central region between the front and back (i.e., two adjacent) PS stripes. The PS latex particles were deposited at the three-phase contact line ("stick"). As the lower substrate was continued moving and water evaporated, the contact angle of the water meniscus was gradually decreased to a critical value, at which the depinning force overcame the pinning force exerted at the contact line.[16c] Thus, the contact line depinned and jumped to the central region between the next two PS stripes (i.e., "slip"), leaving behind colloidal ribbon composed of PS latex particles. The repetitive "stick–slip" motion of the contact line yielded a set of colloidal ribbons situated between PS stripes. Similarly, because of the capillary stress invoked during the drying of the colloidal ribbon, cracks (i.e., microchannels) were formed within each isolated colloidal ribbon and aligned perpendicular to it (Figure S5), that is, oriented parallel to the moving direction of the lower substrate.

When the PS stripe pattern was placed to be parallel to the moving direction of the lower substrate, that is, the PS stripes-deposited Si substrate pattern, the water meniscus of the evaporating droplet containing PS latex particle suspension (0.5 wt %) was greatly curved when it was dragged along the PS stripes due to their strong hydrophobicity, as clearly evident in the representative optical micrograph (Figure S6). The droplet drying led to the formation of intriguing feather-like cracks (i.e., microchannels) between parallel PS stripes (Figure S7). In order to rationalize the formation mechanism of such feather-like microchannels, we first demonstrated that the growth direction of colloidal microchannels was always perpendicular to the three-phase contact line, rather than to the moving direction of the lower substrate. To this end, an angled upper fixed blade with angle $\theta$ of 60° and 30° with respect to the moving direction of the lower Si substrate (without patterned PS stripes on the substrate) was utilized to confine the evaporating droplet (Figures S8,S9). The FESA of the PS latex particle suspension yielded the colloidal microchannels exhibiting a complementary angle $\theta'$ to the moving direction of the lower Si substrate ($\theta' = 90° - \theta = 30°$ in Figure S8b and $\theta' = 90 - \theta = 60°$ in Figure S8c). In addition, multiple generation colloidal cracks (i.e., generational microchannels) were formed using a round-shape upper blade (Figure S9). Thus, the curved three-phase contact line formed as a result of confinement imposed by hydrophobic PS stripes when the PS latex particle water solution was pulled along the PS stripes on the lower Si substrate. As demonstrated in Figures S8,S9, the colloidal microchannels were produced normal to the three-phase contact line (marked as dashed arrows in Figure S6), the feather-like pattern of colloidal microchannels were thus obtained (Figure S6).

The colloidal microchannels can be exploited as a template to pattern nanomaterials (e.g., Au nanoparticles). It is notable that Au nanoparticles (NPs) synthesized by conventional methods usually have an extra amount of ligands in solution and the as-prepared Au NPs are dispersed in aqueous solution.[25] However, as colloidal microchannels composed of PS latex particles are hydrophobic, Au NPs cannot be deposited in the microchannels by water using the Au NPs aqueous solution. To this end, we synthesized PS-capped Au NPs using star-like poly(4-vinylpyridine)-*block*-polystyrene (P4VP-*b*-PS) diblock copolymer as nanoreactor similar to our previous work.[1] The star-like P4VP-*b*-PS formed unimolecular micelles and rendered the preferential incorporation of precursors (i.e., $HAuCl_4$) in the compartment occupied by inner P4VP blocks through strong coordination interaction between the metal ions of precursors and the pyridyl groups of P4VP blocks.[1b,14b] The reduction of $HAuCl_4$ in the presence of reducer (tertbutylamine borane) led to the formation of PS-capped Au NPs. Subsequently, the FESA of PS-capped Au NPs toluene solution (concentration $1 \times 10^{-4}$ M, lower substrate moving speed 100 μm s$^{-1}$) confined between an upper stationary blade and a lower colloidal microchannels-deposited Si substrate was performed. Au NPs were transported by toluene and deposited on the bottom of the microchannels (Figure 4). Surprisingly, instead of fully covering the bottom of microchannels, Au NPs were deposited into two separated threads within a microchannel. This can be

  

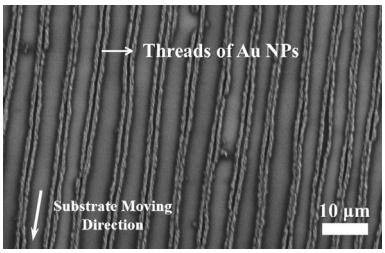


***Figure 4.*** SEM image of aligned threads of Au nanoparticles (NPs) produced by using prepared colloidal cracks (i.e., microchannels) as template.

understood as follows. During the evaporation of the Au NP toluene solution trapped within the microchannel, toluene gradually dewetted from the hydrophilic Si substrate and segregated to the corners on the bottom of microchannels (Figure S10). As a result, Au NPs were positioned at the corners upon the drying of solution. Consequently, inside a microchannel, two parallel threads of Au NPs guided by the shape of microchannel were formed. The Au NP threads-deposited Si substrate was then exposed to oxygen plasma for 1.5 h to remove all residual polymers, forming highly-ordered naked Au NP threads aligned on the Si substrate. It is possible that the Au NPs sintered and consolidated after oxygen plasma treatment.

In summary, we developed a viable flow-enabled self-assembly (FESA) strategy to harness the crack formation which occurred over large areas during the drying of colloidal thin film. The FESA strategy involves the implementation of a restricted geometry composed of an upper stationary blade and a lower movable substrate to confine the drying droplet and control the solvent evaporation. As a result, the generation of cracks in the form of microchannels was effectively tailored. The spacing between two adjacent microchannels ($\lambda_{c-c}$) can be readily tuned by varying the moving velocity of the lower Si substrate ($v$). The relationship between $\lambda_{c-c}$ and $v$ was investigated experimentally and theoretically. In addition, a critical thickness for the formation of microchannels was observed, below which the microchannel-free region appeared periodically in the colloidal thin film. More importantly, the influence of the chemically patterned substrate on the formation of colloidal microchannels was explored. The microchannels were found to be developed in a direction perpendicular to the three-phase contact line. The resulting regularly spaced microchannels can be employed to align nanomaterials guided by the shape of microchannel. The use of FESA strategy for harnessing crack formation that yields highly regular yet tunable structures may provide a unique platform for large-scale manufacturing of crack-based or crack-derived patterns and direct the self-assembly of inorganic nanomaterials for a wide spectrum of applications including optics, electronics, optoelectronics, photonics, microfluidics, sensory materials and device, nanotechnology.

## Acknowledgements

We gratefully acknowledge funding support from NSF (CMMI-1562075). This research was also supported by the BK21 Plus program through the National Research Foundation of Korea funded by the Ministry of Education (grant No. 10Z20130000004 and by National Natural Science Foundation of China (51622301 and 51573046) and Shanghai City 1000 Talent Program.

## Conflict of interest

The authors declare no conflict of interest.

**Keywords:** colloidal particles · cracks · flow-enabled self-assembly · microchannel

**How to cite:** *Angew. Chem. Int. Ed.* **2017**, *56*, 4554 – 4559
*Angew. Chem.* **2017**, *129*, 4625 – 4630

[1] a) X. Pang, Y. He, J. Jung, Z. Lin, *Science* **2016**, *353*, 1268 – 1272; b) X. Pang, L. Zhao, W. Han, X. Xin, Z. Lin, *Nat. Nanotechnol.* **2013**, *8*, 426 – 431.
[2] a) G. M. Whitesides, B. Grzybowski, *Science* **2002**, *295*, 2418 – 2421; b) K. J. M. Bishop, C. E. Wilmer, S. Soh, B. A. Grzybowski, *Small* **2009**, *5*, 1600 – 1630.
[3] a) L. Liao, Y.-C. Lin, M. Bao, R. Cheng, J. Bai, Y. Liu, Y. Qu, K. L. Wang, Y. Huang, X. Duan, *Nature* **2010**, *467*, 305 – 308; b) Z. Nie, A. Petukhova, E. Kumacheva, *Nat. Nanotechnol.* **2010**, *5*, 15 – 25; c) R. D. Piner, J. Zhu, F. Xu, S. Hong, C. A. Mirkin, *Science* **1999**, *283*, 661 – 663.
[4] a) J. Guan, L. J. Lee, *Proc. Natl. Acad. Sci. USA* **2005**, *102*, 18321 – 18325; b) B. Li, W. Han, M. Byun, L. Zhu, Q. Zou, Z. Lin, *ACS Nano* **2013**, *7*, 4326 – 4333.
[5] W. Han, M. Byun, B. Li, X. Pang, Z. Lin, *Angew. Chem. Int. Ed.* **2012**, *51*, 12588 – 12592; *Angew. Chem.* **2012**, *124*, 12756 – 12760.
[6] C. J. Hawker, T. P. Russell, *MRS Bull.* **2005**, *30*, 952 – 966.
[7] a) Y. Jang, J. Jo, D.-S. Kim, *J. Polym. Sci. Part A* **2011**, *49*, 1590 – 1596; b) F. R. Alexander, *Rep. Prog. Phys.* **2013**, *76*, 046603.
[8] a) Z. Néda, K. t. Leung, L. Józsa, M. Ravasz, *Phys. Rev. Lett.* **2002**, *88*, 095502; b) A. T. Ngo, J. Richardi, M. P. Pileni, *Nano Lett.* **2008**, *8*, 2485 – 2489.
[9] a) C. Allain, L. Limat, *Phys. Rev. Lett.* **1995**, *74*, 2981 – 2984; b) E. A. Jagla, *Phys. Rev. E* **2002**, *65*, 046147; c) P. Lidon, J.-B. Salmon, *Soft Matter* **2014**, *10*, 4151 – 4161; d) M. S. Tirumkudulu, W. B. Russel, *Langmuir* **2005**, *21*, 4938 – 4948.
[10] W. Han, B. Li, Z. Lin, *ACS Nano* **2013**, *7*, 6079 – 6085.
[11] Z. Yuan, D. B. Burckel, P. Atanassov, H. Fan, *J. Mater. Chem.* **2006**, *16*, 4637 – 4641.
[12] Y. Lin, E. Balizan, L. A. Lee, Z. Niu, Q. Wang, *Angew. Chem. Int. Ed.* **2010**, *49*, 868 – 872; *Angew. Chem.* **2010**, *122*, 880 – 884.
[13] Z. Lin, S. Granick, *J. Am. Chem. Soc.* **2005**, *127*, 2816 – 2817.
[14] a) H. S. Kim, C. H. Lee, P. K. Sudeep, T. Emrick, A. J. Crosby, *Adv. Mater.* **2010**, *22*, 4600 – 4604; b) B. Li, W. Han, B. Jiang, Z. Lin, *ACS Nano* **2014**, *8*, 2936 – 2942; c) B. Li, C. Zhang, B. Jiang, W. Han, Z. Lin, *Angew. Chem. Int. Ed.* **2015**, *54*, 4250 – 4254; *Angew. Chem.* **2015**, *127*, 4324 – 4328.
[15] D. J. Harris, H. Hu, J. C. Conrad, J. A. Lewis, *Phys. Rev. Lett.* **2007**, *98*, 148301.
[16] a) W. Han, M. He, M. Byun, B. Li, Z. Lin, *Angew. Chem. Int. Ed.* **2013**, *52*, 2564 – 2568; *Angew. Chem.* **2013**, *125*, 2624 – 2628; b) S. W. Hong, J. Xia, Z. Lin, *Adv. Mater.* **2007**, *19*, 1413 – 1417;

  

c) J. Xu, J. Xia, S. W. Hong, Z. Lin, F. Qiu, Y. Yang, *Phys. Rev. Lett.* **2006**, *96*, 066104.
[17] K. Stratford, R. Adhikari, I. Pagonabarraga, J. C. Desplat, M. E. Cates, *Science* **2005**, *309*, 2198.
[18] K. D. M. Rao, R. Gupta, G. U. Kulkarni, *Adv. Mater. Interfaces* **2014**, *1*, 1400090.
[19] R. D. Deegan, O. Bakajin, T. F. Dupont, G. Huber, S. R. Nagel, T. A. Witten, *Nature* **1997**, *389*, 827 – 829.
[20] a) E. R. Dufresne, E. I. Corwin, N. A. Greenblatt, J. Ashmore, D. Y. Wang, A. D. Dinsmore, J. X. Cheng, X. S. Xie, J. W. Hutchinson, D. A. Weitz, *Phys. Rev. Lett.* **2003**, *91*, 224501; b) E. R. Dufresne, D. J. Stark, N. A. Greenblatt, J. X. Cheng, J. W. Hutchinson, L. Mahadevan, D. A. Weitz, *Langmuir* **2006**, *22*, 7144 – 7147; c) J. Ma, G. Jing, *Phys. Rev. E* **2012**, *86*, 061406.
[21] A. F. Routh, W. B. Russel, *Langmuir* **1999**, *15*, 7762 – 7773.
[22] W. P. Lee, A. F. Routh, *Langmuir* **2004**, *20*, 9885 – 9888.
[23] K. B. Singh, M. S. Tirumkudulu, *Phys. Rev. Lett.* **2007**, *98*, 218302.
[24] M. Prasad, M. Kopycinska, U. Rabe, W. Arnold, *Geophys. Res. Lett.* **2002**, *29*, 13-11-13-14.
[25] K. Saha, S. S. Agasti, C. Kim, X. Li, V. M. Rotello, *Chem. Rev.* **2012**, *112*, 2739 – 2779.

Manuscript received: January 14, 2017
Final Article published: March 2, 2017

  